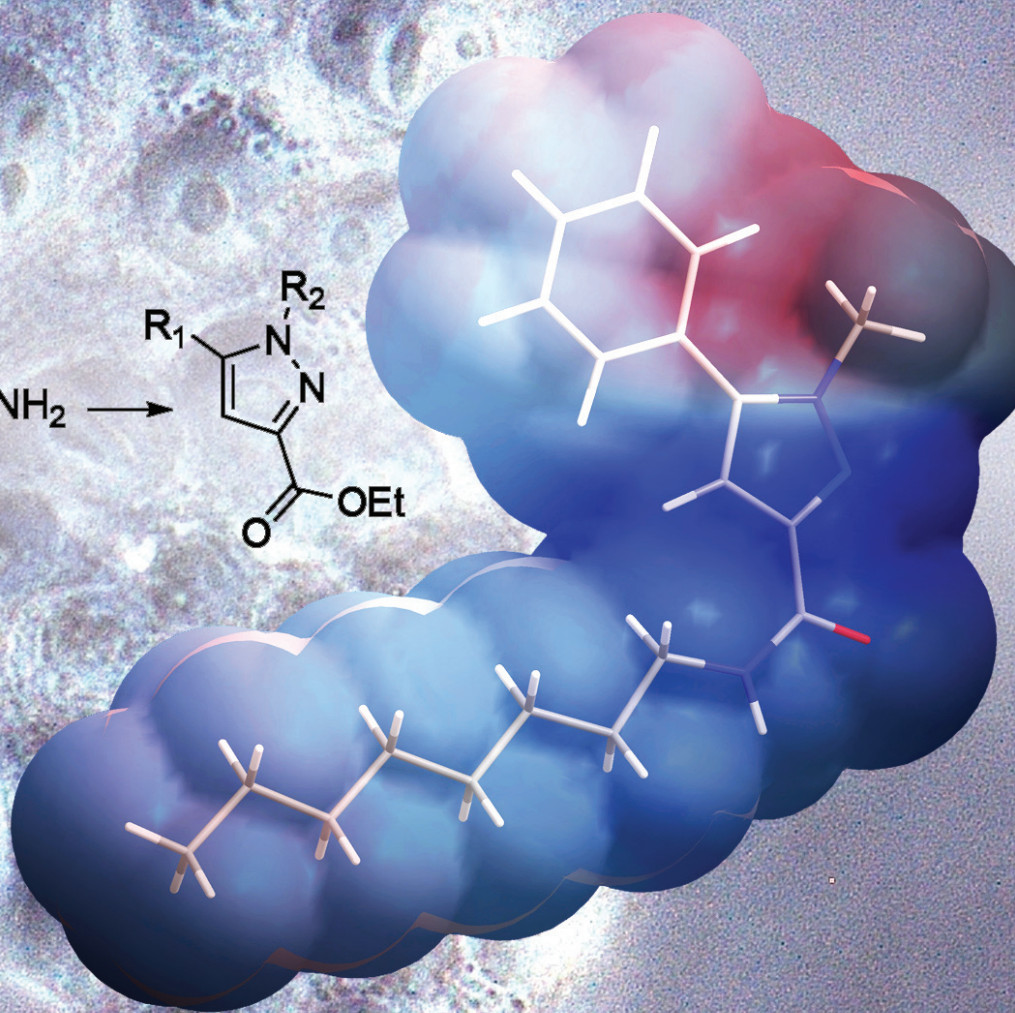
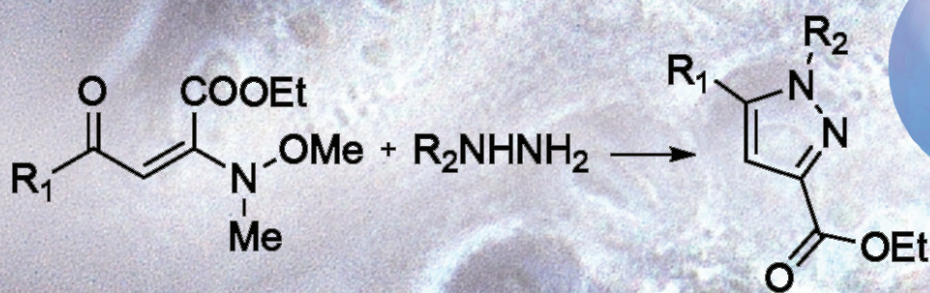


Organic & Biomolecular Chemistry

www.rsc.org/obc

Volume 5 | Number 24 | 21 December 2007 | Pages 3877–4024



ISSN 1477-0520

FULL PAPER

John Nielsen *et al.*

Pyrazole carboxamides and carboxylic acids as protein kinase inhibitors in aberrant eukaryotic signal transduction: induction of growth arrest in MCF-7 cancer cells

Chemical Science

In this issue...



1477-0520(2007)5:24;1-M

RSC Publishing

Pyrazole carboxamides and carboxylic acids as protein kinase inhibitors in aberrant eukaryotic signal transduction: induction of growth arrest in MCF-7 cancer cells

Tobias Persson,^{†a} Christina W. Yde,^b Jakob E. Rasmussen,^a Tine L. Rasmussen,^b Barbara Guerra,^b Olaf-Georg Issinger^b and John Nielsen^{*a}

Received 24th July 2007, Accepted 5th October 2007

First published as an Advance Article on the web 25th October 2007

DOI: 10.1039/b711279c

Densely functionalised pyrazole carboxamides and carboxylic acids were synthesised in an expedient manner through saponification and transamidation, respectively, of ester-functionalised pyrazoles. This synthetic protocol allowed for three diversifying steps in which appendages on the pyrazole scaffold were adjusted to optimise inhibition of protein kinases. Thirty-five analogues were tested in CK2, AKT1, PKA, PKC α , and SAPK2a (p38) kinase inhibition bioassays. Blocking of these kinases may lead to effective therapies for treating inflammatory diseases and cancer. In order to investigate potential biological activity, MCF-7 human breast cancer cells were incubated with the most promising derivatives. Two analogues caused changes in MCF-7 cell growth, one of them through cell cycle arrest demonstrated by cell cycle analysis.

Introduction

All biological functions in eukaryotes are regulated through phosphorylation and dephosphorylation of proteins by protein kinases and protein phosphatases, respectively.¹ The manipulation of these key regulators of cell signalling pathways offers a novel therapeutic approach towards pathological states caused by aberrant eukaryotic signal transduction. The human genome encodes a large number of protein kinases, some recognized as disease-relevant. Despite the ubiquitous nature of the ATP-binding site in protein kinases, selective inhibition of phosphorylation has been demonstrated by small molecules targeting this site.^{2–5} Selective inhibitors can be templated on the same molecular scaffold by optimisation of peripheral groups, the pyrazole skeletal arrangement being a premier kinase-directed privileged structure.^{6–11}

We have selected five representative protein kinases, *i.e.* CK2, AKT1, PKA, PKC α , and SAPK2a (p38) as targets for small molecule intervention. CK2 is known to be elevated in rapidly proliferating tissues and in all currently investigated tumours, where it strongly exhibits anti-apoptotic properties.¹² AKT1 mediates survival signals downstream of PI3-kinase and several growth factor receptors by phosphorylating apoptotic proteins. AKT1 has been shown to be tumourigenic in a mouse lymphoma model and activated and/or overexpressed in a number of cancers, including breast, prostate, lung, pancreatic, liver, ovarian, and colorectal cancers. Moreover, activation of the PI3K/AKT pathway contributes to cisplatin resistance. An analysis of human colorectal cancer for genetic mutations in 340 serine/threonine

kinases revealed mutations in eight genes, including three members of the PI3K pathway. Serine/threonine kinases could therefore serve as sites for therapeutic intervention.¹³ PKA regulates a wide range of cellular processes, including metabolism, gene regulation, cell growth and differentiation.¹⁴ PKC α has been found to be mutated in pituitary and thyroid tumours and deleted in melanoma cell lines. In addition, PKC α is recognized as a therapeutic target in lung, gastric and prostate cancer.¹⁵ Stress-activated protein kinase SAPK2a (p38) belongs to the MAPK family and is activated by a variety of environmental stresses and inflammatory cytokines. SAPK2a has been found to be altered in many cancers and during inflammation.¹⁶ Pyrazole BIRB-796 (Doramapimod, Fig. 1) is a p38 inhibitor¹⁷ in late-stage clinical development phase for the treatment of autoimmune diseases.¹⁸ In MAPK inhibitor SR-144528,¹⁹ the pyrazole moiety of the molecule is the core structure with peripheral groups favouring interactions with a target receptor (Fig. 1).

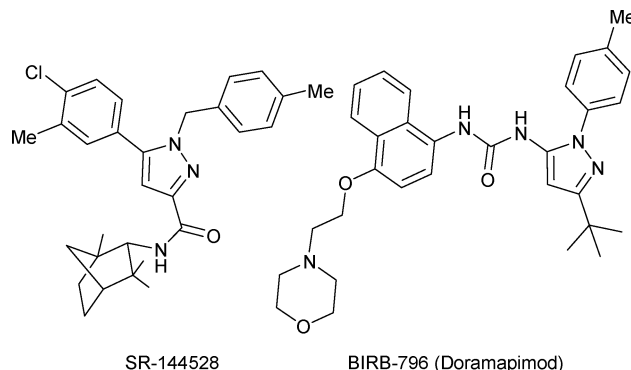


Fig. 1 Molecular structures of SR-144528 and BIRB-796.

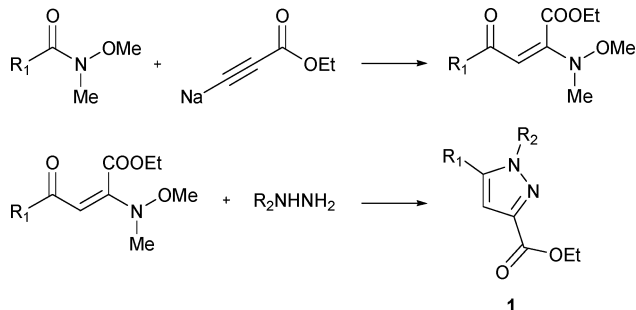
Recently, we reported an acyl substitution–conjugate addition sequence and a regioselective cyclocondensation to yield 1,3,5-trisubstituted pyrazoles in two diversifying steps from a propiolic

^aDepartment of Natural Sciences, Faculty of Life Sciences, University of Copenhagen, Thorvaldsensvej 40, 1871, Frederiksberg, Denmark. E-mail: jn@life.ku.dk; Fax: +45 3533 2398; Tel: +45 3533 2436

^bDepartment of Biochemistry and Molecular Biology, University of Southern Denmark, Denmark

[†]Current address: Department of Medicinal Chemistry, AstraZeneca R & D, Lund, Sweden.

ester, a Weinreb amide and an appropriately substituted hydrazine (Scheme 1).²⁰ Thus, pyrazoles like SR-144528 can be prepared regioselectively from simple and readily available building blocks.



Scheme 1 Synthesis of pyrazole **1** through an acyl substitution–conjugate addition sequence and a cyclocondensation reaction.

Herein, we report our investigation of the acyl substitution–conjugate addition sequence as a platform for appending different building blocks onto the pyrazole scaffold and identification of selective protein kinase inhibitors among compounds that were synthesized.

Results and discussion

The synthetic methodology described in Scheme 1 gave access to the esters **1a–h**, which were subject to further synthetic transformations. Some esters displayed activity in protein kinase inhibition bioassays *per se*, suggesting a complementary biological testing of their carboxylic acid counterparts, since the bioactivity of these esters may depend on enzymatic hydrolysis. Carboxylic acids **2a–g** were synthesised in 58–99% yield (Table 1) by saponification of the corresponding esters (Scheme 2).

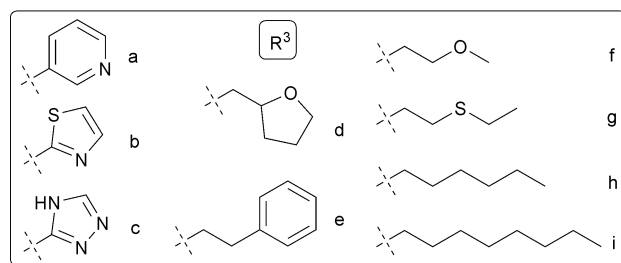
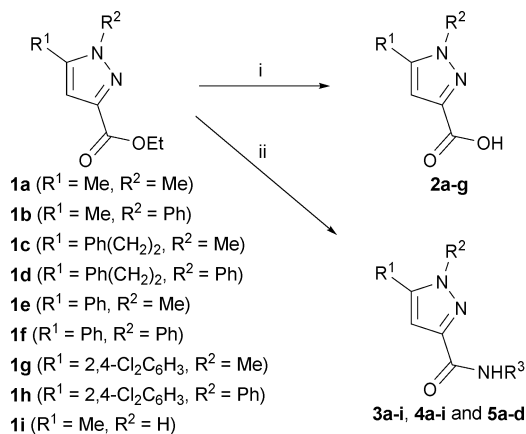
We hypothesised that a more potent protein kinase inhibitor could be identified by the introduction of a third diversity element (R^3 in Scheme 2) to the densely functionalised pyrazole scaffold. This was accomplished by the Weinreb reaction,²¹ converting esters into amides in a single synthetic operation. The mild conditions used originally by Weinreb *et al.*,^{22,23} Me_3Al -mediated transamidation at ambient temperature, applied well to the synthesis of **3e–i** and **4e–i** but not to reactions involving heterocyclic primary amines (synthesis of **3a–d** and **4a–d** was unsuccessful with method A). Even at 50 °C in THF, 1,4-dioxane or DMF, the formation of **5b** could not be observed. However, only the synthesis of **4a–c** remained unsuccessful, when the reactions were run according to a modified protocol, method B, in pyridine at 50 °C. Except for products **3a**, **3c**, **5b** and **5c** for which yields were still on the low side, the transamidation reactions worked satisfyingly with yields in the range of 41–92% employing either method A or B (Table 1).

Compounds **1a–h**, **2a–g**, **3a**, **3c–i**, **4d–i** and **5a–d** were tested on selected kinase targets AKT1, CK2, PKA and p38 for their ability to serve as protein kinase inhibitors. Each compound was tested at a final concentration of 10 μM . Table 2 shows the results obtained as the percentage of protein kinase activity remaining. Compound **1f** displayed a significant inhibition of AKT1 and SAPK2a (p38) kinases, reducing the kinase activity by 40% and 35%, respectively. Compound **1e** also inhibited AKT1 kinase, although only by 26%. A 65% inhibition of PKA activity was caused by compound **1a**. Compound **2e** inhibited AKT1 by 46%

Table 1 Synthesis of **2a–g** through saponification and **3a**, **3c–i**, **4d–i** and **5a–d** through transamidation of **1b–h**

Starting material	R^1	R^2	R^3	Product	Yield (%) ^a	Method
1b	Me	Ph	—	2a	99	—
1c	$\text{Ph}(\text{CH}_2)_2$	Me	—	2b	82	—
1d	$\text{Ph}(\text{CH}_2)_2$	Ph	—	2c	77	—
1e	Ph	Me	—	2d	67	—
1f	Ph	Ph	—	2e	58	—
1g	2,4- $\text{Cl}_2\text{C}_6\text{H}_3$	Me	—	2f	58	—
1h	2,4- $\text{Cl}_2\text{C}_6\text{H}_3$	Ph	—	2g	81	—
1a	Me	Me	a	3a	32	B
1a	Me	Me	b	3b	— ^b	B
1a	Me	Me	c	3c	26	B
1a	Me	Me	d	3d	85	B
1a	Me	Me	e	3e	55	A
1a	Me	Me	f	3f	49	A
1a	Me	Me	g	3g	62	A ^d
1a	Me	Me	h	3h	59	A
1a	Me	Me	i	3i	63	A
1e	Ph	Me	a	4a	— ^c	B
1e	Ph	Me	b	4b	— ^c	B
1e	Ph	Me	c	4c	— ^c	B
1e	Ph	Me	d	4d	41	B ^e
1e	Ph	Me	e	4e	52	A
1e	Ph	Me	f	4f	72	A
1e	Ph	Me	g	4g	58	A ^d
1e	Ph	Me	h	4h	59	A
1e	Ph	Me	i	4i	72	A
1i	Me	H	a	5a	92	B
1i	Me	H	b	5b	32	B
1i	Me	H	c	5c	23	B
1i	Me	H	d	5d	80	B

^a Isolated yields after purification by preparative RP-HPLC. ^b Inseparable mixture of products and starting material. ^c No reaction observed. ^d Addition of DIPEA (3.1 eq.). ^e 0 °C \rightarrow rt.



Scheme 2 Reagents and conditions: (i) LiOH, THF– H_2O , rt; (ii) $\text{R}^3\text{-NH}_2$, Me_3Al , 0 °C \rightarrow rt in CHCl_3 (method A) or 0 °C \rightarrow 50 °C in py (method B).

Table 2 Inhibition of AKT1, CK2, PKA, PKC α and p38 kinase activity by compounds **1a–h**, **2a–g**, **3a**, **3c–i**, **4d–i** and **5a–d**^a

Compound	AKT1	CK2	PKA	PKC α	p38
1a	65	76	35	—	101
1b	122	98	84	101	107
1c	108	109	96	98	96
1d	90	102	104	100	100
1e	74	100	119	98	95
1f	60	102	80	86	65
1g	99	106	81	99	92
1h	81	97	60	96	97
2a	70	66	14	—	92
2b	45	78	40	—	87
2c	61	75	37	—	98
2d	62	78	36	—	79
2e	54	69	18	—	90
2f	59	77	39	—	73
2g	54	85	34	—	80
3a	78	80	29	—	86
3c	67	86	86	—	82
3d	52	87	44	—	91
3e	80	78	61	—	87
3f	100	89	96	—	84
3g	88	89	86	—	91
3h	48	89	49	—	94
3i	83	77	57	—	100
4d	46	84	39	—	84
4e	80	82	29	—	86
4f	73	84	46	—	94
4g	75	80	44	—	88
4h	72	70	28	—	99
4i	39	58	16	—	92
5a	82	78	38	—	70
5b	69	73	43	—	108
5c	66	73	23	—	94
5d	60	80	32	—	77

^a Kinase activity tests were performed using recombinant AKT1, CK2, PKA, PKC α and p38. Values in the table are calculated as the remaining kinase activity in % of control (no inhibitor) after incubation with 10 μ M of each of the indicated compounds for 10 min at 30 °C.

and PKA by 82%, while **4i** inhibited AKT1, CK2 and PKA by 61%, 42% and 84%, respectively. It is interesting to note the structural difference between the most potent p38 inhibitor in this investigation, **1f**, and for example that of BIRB-796, which is a potent well-investigated p38 inhibitor.²⁴ The substitution pattern in compound **1f**, with a H-bond donor/acceptor in the 3-position and a lipophilic group in the 5-position, is opposite to that in BIRB-796.

In order to explore the potential biological activity of compounds **1f**, **2e** and **4i** further, we incubated MCF-7 human breast cancer cells with the aforementioned inhibitors at concentrations of 50 and 100 μ M, respectively, for 48 h. Analysis of the cells by phase-contrast microscopy revealed that the treatment with **1f** and **4i** had a clear inhibitory effect on cell growth as compared to the control experiment. The effect was markedly visible at a concentration of 100 μ M (Fig. 2). Cell treatment with **2e** did not cause changes in cell growth.

In order to determine the effect of the selected inhibitors on cell growth more quantitatively, cells were scored for viability by the crystal violet binding method. As shown in Fig. 3, incubation of cells for up to 72 h with **2e** at concentrations of 50 and 100 μ M, respectively, did not lead to a significant change in cell viability as compared with control cells. Treatment with **1f** led to a ~50%

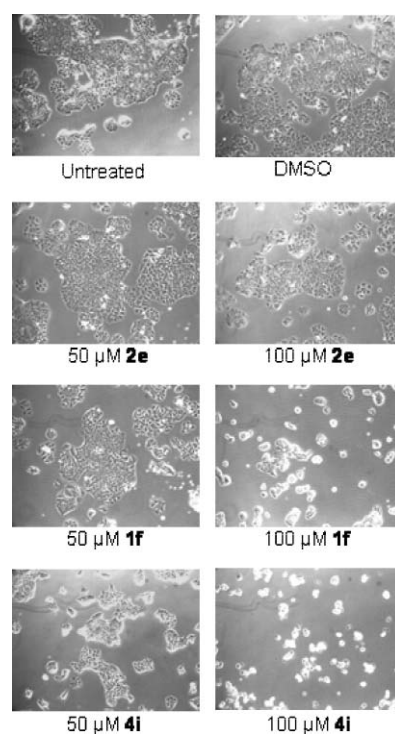


Fig. 2 MCF-7 cells were either untreated or incubated with the indicated inhibitors for 48 h at a concentration as entered of 50 μ M and 100 μ M, respectively. Control cells were treated with DMSO. Morphological effects of the different compounds were examined by phase-contrast microscopy. Data shown are representative of three independent experiments.

decrease in viability after 24 h of incubation. Only with the highest concentration applied (*i.e.* 100 μ M) was a further decrease in the percentage of viable cells after 72 h of incubation observed (24% of cells remaining). The treatment of cells with **4i** resulted in a marked decrease in viable cells, which was substantial when cells were incubated with 100 μ M **4i** for 72 h (10% cells remaining).

Next, we analyzed the distribution of the cells in the different phases of the cell cycle before and after treatment with the aforementioned compounds for 24 h (data not shown) and 48 h (Fig. 4). The incubation of MCF-7 cells with 100 μ M **1f** and **2e** for up to 48 h did not cause any variation in cell cycle distribution as compared to control cells. Interestingly, the treatment with **4i** for 48 h caused cell cycle arrest in the S (the percentage varied from 7.7 in control cells to 20.3 in treated cells) and G2/M (the percentage increased from 11.1 in control cells to 22.4 in treated cells) phases.

We wanted to evaluate the physiological effect of the three inhibitors **1f**, **2e** and **4i** using the human breast cancer cell line MCF-7. Different methods were conducted in order to investigate morphological changes and effects on cell viability and cell cycle distribution. Compounds **1f** and **4i** clearly affected MCF-7 cells at concentrations of 50 and 100 μ M, resulting in reduced cell numbers being observed when evaluating cells under phase-contrast microscopy as well as by quantifying cells by crystal violet staining. Compound **2e**, on the other hand, did not affect cell morphology or viability. None of the compounds seemed to cause severe cell death as we did not observe high numbers of floating dead cells under the microscope.

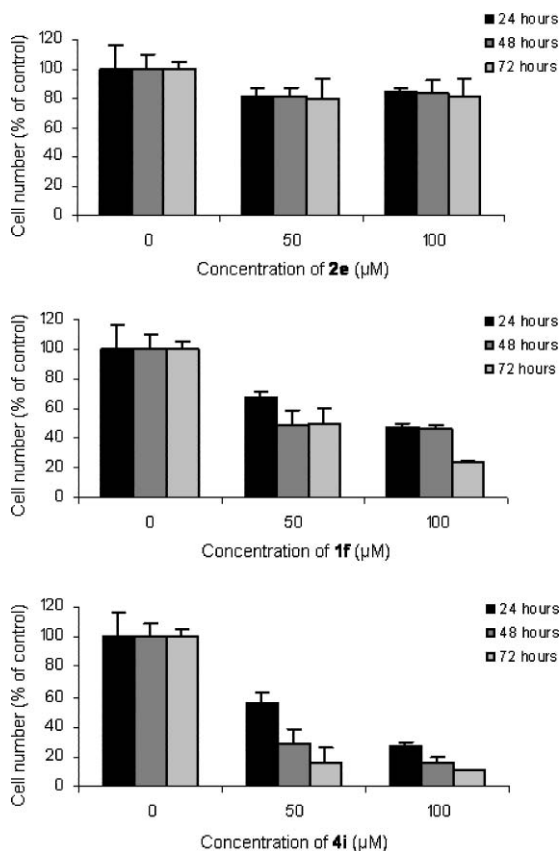


Fig. 3 MCF-7 cells were seeded in 96-well plates and after 24 h cells were incubated with 50 and 100 μM of **2e**, **1f** and **4i** as indicated in the figure. Cell viability was assessed by staining the cells with crystal violet as described in the Experimental section. The number of viable cells is expressed as a percentage, assigning a value of 100 to the cells treated with DMSO only (control). Data were generated in triplicate and are shown as the average value \pm standard deviation.

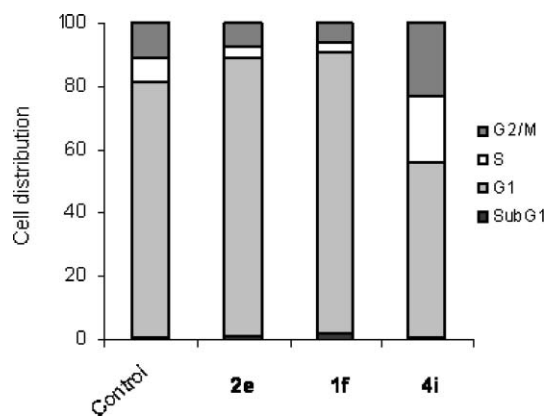


Fig. 4 MCF-7 cells were incubated with the indicated compounds for 48 h. Control cells were incubated with an equivalent amount of DMSO. Cells were harvested, fixed, stained with propidium iodide and analysed by flow cytometry. The percentage of cells in each phase of the cell cycle (*i.e.* sub-G1, G1, S and G2/M) is indicated. Data are representative of two experiments performed independently.

Since the crystal violet staining does not distinguish between actively dividing cells or quiescent cells, the reduced cell number can be both a result of cytotoxic and cytostatic effects. We

performed cell cycle analysis in order to see if any of the inhibitors caused cell cycle arrest. We found that only **4i** resulted in accumulation in S- and G2/M-cell cycle phases. Therefore the reduced cell number after treatment with **4i** observed in the crystal violet assay might be a result of arrested cells. Compound **1f** did not cause cells to arrest in any of the cell cycle phases. It can therefore be speculated that **1f** slows down cell metabolism, thereby making the cells grow more slowly. The kinase activity tests showed that **1f** inhibits the protein kinases p38 MAPK and AKT1. AKT is involved in cell-cycle progression, inhibition of apoptosis and transcriptional control.²⁵ A drug targeting AKT is expected to affect cell growth and viability, and therefore the kinetic data fit well with the biological observations. Compound **4i** inhibits several kinases in our kinase assay including CK2, AKT and PKA. This indicates that the inhibitor is a multi-targeting inhibitor, and we observed that treatment with the compound reduces cell viability, presumably by cell cycle arrest. Further experiments, however, are needed in order to elucidate the exact mechanisms of growth inhibition by the compounds **1f** and **4i**.

Conclusions

An expedient synthetic approach to densely functionalised pyrazoles allowed for the synthesis of a combinatorial array of pyrazole carboxylic acid and carboxamide derivatives. The focused library of pyrazoles furnished several promising protein kinase inhibitors in AKT1, CK2, PKA and p38 kinase inhibition assays. Most prominent were the identified inhibitors of AKT1 and PKA kinases.

Two of the three most promising derivatives, namely compounds **1f** and **4i**, demonstrated great promise against MCF-7 breast cancer cells. The third derivative, ester **2e**, did not cause changes in MCF-7 cancer cell growth but was more potent than carboxylic acid **1f** in cell free assays. This duality may be caused by esterase activity in cells and, as a consequence, changing bioavailability of the former. The cell cycle arrest observed in MCF-7 breast cancer cells after incubation with carboxamide **4i**, exposing a lipophilic appendage, was the most promising demonstration of inhibitory activity.

Experimental

Kinase inhibition assay

Protein kinases were obtained from KinaseDetect ApS and tested according to the manufacturers recommendations (<http://www.kinasedetect.dk/>). For all tests a general procedure was chosen: Reactions were performed in a 40 μL assay volume. 10 μL buffer, 10 μL substrate and enzyme were pipetted in, followed by the addition of the inhibitor (diluted in buffer or DMSO to a final concentration of 10 μM). The reaction was started by the addition of [γ -³²P]-ATP to a final concentration of 125 μM . Incubation was for 10 min at 30 $^{\circ}\text{C}$ in a water bath. The reaction was stopped by transferring the samples to an ice bath. Then 10 μL aliquots were spotted on P81 Whatman filter squares washed three times in phosphoric acid. The filters were dried and counted in a liquid scintillation counter.

The first screening for kinase inhibition was performed once in duplicate for each kinase activity test. In case of inhibition in the

first screening, the test was repeated 3 times. The background was subtracted from all values. The control (no inhibitor) was set at 100%, and the calculated value obtained in the presence of the inhibitor was presented as remaining activity.

Cell culture and treatments

The MCF-7 cell line was grown in Roswell Park Memorial Institute medium (RPMI, Gibco), supplemented with 10% (v/v) fetal bovine serum (FBS) and 1 mM L-glutamine. Cells were cultured at 37 °C in a humidified 5% CO₂ incubator. For drug treatment, cells were seeded in tissue culture dishes 24 h prior to treatment with 50 or 100 μM **1f**, **2e** and **4i**, respectively, for the times indicated in the figure legends. Control cells were treated with an equivalent amount of DMSO.

Cell cycle analysis

Treated cells were harvested by trypsinisation, washed extensively with phosphate-buffered saline (PBS) and fixed with ice-cold 70% ethanol overnight at –20 °C. Fixed cells were then resuspended in PBS containing 40 μg mL⁻¹ RNase and 20 μg mL⁻¹ propidium iodide (both from Sigma) for 30 min at room temperature prior to analysis. The DNA content was analysed by Flow Cytometry (FACSCalibur, Becton Dickinson Biosciences). Acquired data from 10 000 events were processed by Cell Quest Pro analysis software.

Colorimetric growth assay by the crystal violet staining method

For determination of cell viability, cells were treated with the inhibitors, and the cell number was evaluated by a crystal violet colorimetric assay. Briefly, cells were stained with a solution of 0.5% crystal violet in 25% methanol for 10 min, after which excess stain was washed away with H₂O. Crystal violet dye bound to cells was resuspended in a solution of 0.1 M sodium citrate in 50% ethanol, and the absorbance at 570 nm was measured in a plate reader (VERSAmax, Molecular Devices).

General experimental information

Commercially available reagents (Aldrich) were used without further purification unless otherwise noted. Compound **1i** (R¹ = Me, R² = H) was purchased from Aldrich, and starting materials **1a–h** were prepared as previously reported.²⁰ Solvents used for the synthesis were of analytical grade, dried over activated 4 Å molecular sieves when necessary (all solvents used under dry conditions had a water content <25 ppm measured by Karl-Fischer titration). All reactions employing Me₃Al as reagent were performed under dry conditions in an atmosphere of argon (dried by passage through phosphorus pentoxide). Analytical TLC was performed using pre-coated silica gel 60 F₂₅₄ plates and visualised using either UV light, phosphomolybdic acid or potassium permanganate stain. Parallel reactions requiring cooling were performed in a Radley Greenhouse Parallel Synthesizer™ block. Corrected melting points were measured on a Reichert melting point microscope, number N254-1R. ¹H and ¹³C NMR spectral data were recorded on a Bruker Avance 300 spectrometer using the deuterated solvent as lock. Chemical shifts are reported in ppm relative to the residual solvent peak (¹H NMR) or the

solvent peak (¹³C NMR) as the internal standard. *J* values are given in Hz. Accurate mass determinations were performed on a Micromass LCT apparatus equipped with an AP-ESI probe calibrated with Leu-Enkephalin (556.2771 u). MilliQ water was used for RP-HPLC. RP-HPLC was performed on a Waters 2525 system equipped with a Waters 2996 photodiode array detector and Phenomenex C18 columns (analytical: 4.6 × 100 mm, 5 μm) or Xterra C18 columns (preparative: 19 × 100 mm, 5 μm) with a flow of 1.5 mL min⁻¹ (5% → 100% CH₃CN in H₂O for 7 min) and 15 mL min⁻¹ (compounds **2a–g**: 45% → 65% CH₃CN in H₂O for 7 min; compounds **3a**, **3c–i**, **4d–i** and **5a–d**: 5% → 100% CH₃CN in 0.1% aq. TFA for 9 min), respectively. Purity determinations of all compounds tested in bioassays were made by analytical RP-HPLC (220 nm).

General procedure for synthesis of 2a–g

Ester **1** was dissolved in THF (0.1 M) and 1 M LiOH (aq., 1.1 eq.) added. The resulting suspension was stirred at rt for 19 h and completion of the reaction was observed by analytical RP-HPLC. Volatiles were removed at reduced pressure, and the residue was acidified with 1 M KHSO₄ (aq.). The resulting suspension was dissolved in least amount of CH₃CN–DMSO, and the product was isolated by preparative RP-HPLC.

5-Methyl-1-phenyl-1H-pyrazole-3-carboxylic acid (2a). Compound **1b** (4.5 mg, 0.020 mmol) yielded **2a** (4.0 mg, 99%, UV purity: 97%) as a colourless solid: Mp 127–129 °C (lit.²⁶ mp 132–133 °C); ¹³C NMR (75 MHz, CDCl₃) δ 165.1, 142.7, 141.5, 138.8, 129.2, 128.8, 125.2, 109.0, 12.4; HRMS (M + H)⁺ calcd. for C₁₁H₁₁N₂O₂⁺ 203.0821, found 203.0831. ¹H NMR spectroscopic data were in agreement with those previously reported.²⁷

1-Methyl-5-phenylethyl-1H-pyrazole-3-carboxylic acid (2b). Compound **1c** (9.6 mg, 0.037 mmol) yielded **2b** (7.0 mg, 82%, UV purity: 99%) as a colourless solid: Mp 152–153 °C; ¹H NMR (300 MHz, CDCl₃) δ 7.33–7.13 (m, 5 H), 6.68 (s, 1 H), 3.70 (s, 3 H), 3.00–2.91 (m, 4 H); ¹³C NMR (75 MHz, CDCl₃) δ 165.2, 144.4, 141.2, 139.9, 128.6, 128.3, 126.6, 107.7, 36.8, 34.8, 27.6; HRMS (M + H)⁺ calcd. for C₁₃H₁₅N₂O₂⁺ 231.1134, found 231.1138.

1-Phenyl-5-phenylethyl-1H-pyrazole-3-carboxylic acid (2c). Compound **1d** (10 mg, 0.032 mmol) yielded **2c** (7.2 mg, 77%, UV purity: 97%) as a colourless solid: Mp 114–115 °C; ¹H NMR (300 MHz, CDCl₃) δ 7.49–7.04 (m, 10 H), 6.85 (s, 1 H), 3.00–2.87 (m, 4 H); ¹³C NMR (75 MHz, CDCl₃) δ 164.0, 145.5, 142.8, 139.9, 138.8, 129.2, 129.0, 128.5, 128.2, 126.5, 125.7, 108.1, 34.8, 28.0; HRMS (M + H)⁺ calcd. for C₁₈H₁₇N₂O₂⁺ 293.1290, found 293.1302.

1-Methyl-5-phenyl-1H-pyrazole-3-carboxylic acid (2d). Compound **1e** (13 mg, 0.056 mmol) yielded **2d** (7.6 mg, 67%, UV purity: 74%) as a colourless solid: Mp 134–136 °C (lit.²⁸ mp 143–145 °C); ¹³C NMR (75 MHz, CDCl₃) δ 165.1, 145.6, 141.6, 129.3, 129.2, 128.9, 128.8, 109.1, 38.3; HRMS (M + H)⁺ calcd. for C₁₁H₁₁N₂O₂⁺ 203.0821, found 203.0817. ¹H NMR spectroscopic data were in agreement with those previously reported.²⁸

1,5-Diphenyl-1H-pyrazole-3-carboxylic acid (2e). Compound **1f** (15 mg, 0.051 mmol) yielded **2e** (7.8 mg, 58%, UV purity: 85%) as a colourless solid: Mp 171–173 °C (lit.²⁹ mp 185 °C); ¹H NMR (300 MHz, CDCl₃) δ 7.39–7.21 (m, 10 H), 7.10 (s, 1 H); ¹³C NMR

(75 MHz, CDCl₃) δ 164.2, 145.4, 143.1, 139.3, 129.2, 129.0, 128.9, 128.7, 128.6, 128.5, 125.5, 109.9; HRMS (M + H)⁺ calcd. for C₁₆H₁₃N₂O₂⁺ 265.0977, found 265.0975.

1-Methyl-5-(2,4-dichlorophenyl)-1H-pyrazole-3-carboxylic acid (2f). Compound **1g** (13 mg, 0.043 mmol) yielded **2f** (6.8 mg, 58%, UV purity: 99%) as a colourless solid: Mp 167–168 °C; ¹H NMR (300 MHz, CDCl₃) δ 7.57 (d, 1 H, *J* 2.0), 7.39 (dd, 1 H, *J* 8.3 and 2.0), 7.29 (d, 1 H, *J* 8.3), 6.88 (s, 1 H), 3.80 (s, 3 H); ¹³C NMR (75 MHz, CDCl₃) δ 163.6, 141.6, 141.5, 136.7, 135.2, 132.6, 130.0, 127.5, 127.1, 110.4, 37.9; HRMS (M + H)⁺ calcd. for C₁₁H₉Cl₂N₂O₂⁺ 271.0041, found 271.0052.

1-Phenyl-(2,4-dichlorophenyl)-1H-pyrazole-3-carboxylic acid (2g). Compound **1h** (9.2 mg, 0.026 mmol) yielded **2g** (7.0 mg, 81%, UV purity: 82%) as a colourless solid: Mp 190–192 °C; ¹H NMR (300 MHz, CDCl₃) δ 7.44–7.17 (m, 8 H), 7.10 (s, 1 H); ¹³C NMR (75 MHz, CDCl₃) δ 163.2, 143.1, 141.0, 139.0, 136.3, 134.8, 132.7, 130.1, 129.1, 128.5, 127.4, 127.3, 124.5, 111.9; HRMS (M + H)⁺ calcd. for C₁₆H₁₁N₂O₂Cl₂⁺ 333.0198, found 333.0218.

General procedure for synthesis of 3e–i and 4e–i (Method A)

A 2 M hexane solution of Me₃Al (3 eq.) was added dropwise *via* syringe to a CHCl₃ solution (2 mL) of amine (3 eq. R³–NH₂, amines used in the synthesis of **3g** and **4g** were supplied as HCl salts dissolved by addition of 3.1 eq. DIPEA) cooled at 0 °C under dry conditions. The ice bath was removed, and the reaction mixture was stirred at rt for 2 h. Ester **1a** or **1e** (1 eq.) was dissolved in CHCl₃ (0.2 mL) and added *via* micropipette. After 96 h stirring at rt the reaction was quenched by addition of 0.67 M HCl (aq.). The crude mixtures were filtered through basic alumina, and the filtrate was evaporated to dryness at reduced pressure. The products were isolated by preparative RP-HPLC.

1,5-Dimethyl-N-phenethyl-1H-pyrazole-3-carboxamide (3e). Compound **1a** (19 mg, 0.113 mmol) yielded **3e** (15 mg, 55%, UV purity: 96%) as a colourless solid: Mp 107–109 °C; ¹H NMR (300 MHz, CDCl₃) δ 7.33–7.22 (m, 5 H), 6.95 (br s, 1 H), 6.54 (s, 1 H), 3.75 (s, 3 H), 3.66 (q, 2 H, *J* 7.2), 2.90 (t, 3 H, *J* 7.2), 2.28 (s, 3 H); ¹³C NMR (75 MHz, CDCl₃) δ 162.5, 144.9, 140.5, 139.1, 128.9, 128.7, 126.5, 106.3, 40.6, 36.6, 36.1, 11.4; HRMS (M + H)⁺ calcd. for C₁₄H₁₈N₃O⁺ 244.1444, found 244.1434.

N-(2-Methoxyethyl)-1,5-dimethyl-1H-pyrazole-3-carboxamide (3f). Compound **1a** (19 mg, 0.113 mmol) yielded **3f** (11 mg, 49%, UV purity: 97%) as a colourless solid: Mp 61–64 °C; ¹H NMR (300 MHz, CDCl₃) δ 7.14 (br s, 1 H), 6.53 (s, 1 H), 3.77 (s, 3 H), 3.62–3.52 (m, 4 H), 3.38 (s, 3 H), 2.28 (s, 3 H); ¹³C NMR (75 MHz, CDCl₃) δ 162.5, 144.9, 140.2, 106.1, 71.4, 58.8, 38.8, 36.5, 11.3; HRMS (M + H)⁺ calcd. for C₉H₁₆N₃O₂⁺ 198.1237, found 198.1232.

N-(2-(Ethylthio)ethyl)-1,5-dimethyl-1H-pyrazole-3-carboxamide (3g). Compound **1a** (19 mg, 0.113 mmol) yielded **3g** (16 mg, 62%, UV purity: 93%) as a colourless oil; ¹H NMR (300 MHz, CDCl₃) δ 7.16 (br s, 1 H), 6.52 (s, 1 H), 3.77 (s, 3 H), 3.59 (q, 2 H, *J* 6.6), 2.74 (t, 2 H, *J* 6.6), 2.58 (q, 2 H, *J* 7.5), 2.27 (s, 3 H), 1.26 (t, 3 H, *J* 7.5); ¹³C NMR (75 MHz, CDCl₃) δ 162.5, 145.0, 140.4, 106.2, 38.5, 36.7, 31.5, 25.8, 14.9, 11.4; HRMS (M + H)⁺ calcd. for C₁₀H₁₈N₃OS⁺ 228.1165, found 228.1176.

N-Hexyl-1,5-dimethyl-1H-pyrazole-3-carboxamide (3h). Compound **1a** (19 mg, 0.113 mmol) yielded **3h** (15 mg, 59%, UV purity: 97%) as a colourless oil; ¹H NMR (300 MHz, CDCl₃) δ 6.82 (br s, 1 H), 6.53 (s, 1 H), 3.77 (s, 3 H), 3.38 (q, 2 H, *J* 6.6), 2.27 (s, 3 H), 1.62–1.53 (m, 2 H), 1.42–1.20 (m, 12 H), 0.87 (t, 3 H, *J* 6.6); ¹³C NMR (75 MHz, CDCl₃) δ 162.4, 145.3, 140.4, 106.2, 39.3, 36.6, 31.7, 29.8, 26.8, 22.7, 14.2, 11.4; HRMS (M + H)⁺ calcd. for C₁₂H₂₂N₃O⁺ 224.1757, found 224.1777.

1,5-Dimethyl-N-octyl-1H-pyrazole-3-carboxamide (3i). Compound **1a** (19 mg, 0.113 mmol) yielded **3i** (18 mg, 63%, UV purity: 98%) as a colourless oil; ¹H NMR (300 MHz, CDCl₃) δ 6.82 (br s, 1 H), 6.53 (s, 1 H), 3.77 (s, 3 H), 3.38 (q, 2 H, *J* 6.6), 2.27 (s, 3 H), 1.62–1.52 (m, 2 H), 1.41–1.18 (m, 10 H), 0.87 (t, 3 H, *J* 6.6); ¹³C NMR (75 MHz, CDCl₃) δ 162.4, 145.3, 140.4, 106.2, 39.3, 36.6, 31.9, 29.9, 29.4, 29.3, 27.1, 22.8, 14.2, 11.4; HRMS (M + H)⁺ calcd. for C₁₄H₂₆N₃O⁺ 252.2070, found 252.2090.

1-Methyl-N-phenethyl-5-phenyl-1H-pyrazole-3-carboxamide (4e). Compound **1e** (20 mg, 0.089 mmol) yielded **4e** (14 mg, 52%, UV purity: 97%) as a colourless solid: Mp 128–129 °C; ¹H NMR (300 MHz, CDCl₃) δ 7.50–7.39 (m, 5 H), 7.35–7.21 (m, 5 H), 7.00 (br s, 1 H), 6.84 (s, 1 H), 3.86 (s, 3 H), 3.70 (q, 2 H, *J* 6.9), 2.94 (t, 2 H, *J* 7.2); ¹³C NMR (75 MHz, CDCl₃) δ 162.2, 145.6, 139.2, 129.1–128.7 (10C), 129.9, 126.6, 106.9, 40.6, 38.1, 36.2; HRMS (M + H)⁺ calcd. for C₁₉H₂₀N₃O⁺ 306.1601, found 306.1595.

N-(2-Methoxyethyl)-1-methyl-5-phenyl-1H-pyrazole-3-carboxamide (4f). Compound **1e** (20 mg, 0.089 mmol) yielded **4f** (17 mg, 72%, UV purity: 93%) as a colourless oil; ¹H NMR (300 MHz, CDCl₃) δ 7.50–7.38 (m, 5 H), 7.21 (br s, 1 H), 6.83 (s, 1 H), 3.88 (s, 3 H), 3.64 (m, 2 H, *J* 5.4), 3.56 (t, 2 H, *J* 4.8), 3.40 (s, 3 H); ¹³C NMR (75 MHz, CDCl₃) δ 162.3, 145.6, 130.1, 129.0–128.9 (6C), 106.8, 71.5, 59.0, 39.0, 38.1; HRMS (M + H)⁺ calcd. for C₁₄H₁₈N₃O₂⁺ 260.1394, found 260.1416.

N-(2-(Ethylthio)ethyl)-1-methyl-5-phenyl-1H-pyrazole-3-carboxamide (4g). Compound **1e** (20 mg, 0.089 mmol) yielded **4g** (15 mg, 58%, UV purity: 75%) as a colourless solid: Mp 66–68 °C; ¹H NMR (300 MHz, CDCl₃) δ 7.50–7.39 (m, 5 H), 7.25 (br s, 1 H), 6.83 (s, 1 H), 3.89 (s, 3 H), 3.64 (q, 2 H, *J* 6.3), 2.78 (t, 2 H, *J* 6.6), 2.61 (q, 2 H, *J* 7.2), 1.29 (t, 3 H, *J* 7.5); ¹³C NMR (75 MHz, CDCl₃) δ 162.1, 145.5, 129.9, 129.1–128.9 (6C), 106.9, 38.6, 38.1, 31.6, 25.9, 15.0; HRMS (M + H)⁺ calcd. for C₁₅H₂₀N₃OS⁺ 290.1322, found 290.1317.

N-Hexyl-1-methyl-5-phenyl-1H-pyrazole-3-carboxamide (4h). Compound **1e** (20 mg, 0.089 mmol) yielded **4h** (15 mg, 59%, UV purity: 93%) as a colourless solid: Mp 48–51 °C; ¹H NMR (300 MHz, CDCl₃) δ 7.50–7.39 (m, 5 H), 6.89 (br s, 1 H), 6.83 (s, 1 H), 3.88 (s, 3 H), 3.43 (q, 2 H, *J* 6.6), 1.66–1.56 (m, 2 H), 1.44–1.25 (m, 6 H), 0.89 (t, 3 H, *J* 7.2); ¹³C NMR (75 MHz, CDCl₃) δ 162.1, 145.9, 145.5, 130.1, 129.0–128.9 (5C), 106.8, 39.3, 38.1, 31.7, 29.9, 26.8, 22.7, 14.2; HRMS (M + H)⁺ calcd. for C₁₇H₂₄N₃O⁺ 286.1914, found 286.1906.

1-Methyl-N-octyl-5-phenyl-1H-pyrazole-3-carboxamide (4i). Compound **1e** (20 mg, 0.089 mmol) yielded **4i** (20 mg, 72%, UV purity: 92%) as a colourless oil; ¹H NMR (300 MHz, CDCl₃) δ 7.50–7.38 (m, 5 H), 6.90 (br s, 1 H), 6.84 (s, 1 H), 3.88 (s, 3 H), 3.43 (q, 2 H, *J* 6.7), 1.64–1.57 (m, 2 H), 1.43–1.22 (m, 10 H), 0.88 (t, 3 H, *J* 6.9); ¹³C NMR (75 MHz, CDCl₃) δ 162.2, 145.8,

145.5, 130.1, 129.0–128.9 (5C), 106.80, 39.4, 38.1, 32.0, 29.9, 29.4, 29.3, 27.1, 22.8, 14.2; HRMS (M + H)⁺ calcd. for C₁₉H₂₈N₃O⁺ 314.2227, found 314.2209.

General procedure for synthesis of 3a, 3c, 3d, 4d, and 5a–d (Method B)

While cooling a pyridine solution (1 mL) of amine (3 eq. R³–NH₂) at 0 °C under dry conditions, a 2 M hexane solution of Me₃Al (3 eq.) was added dropwise *via* syringe. The ice bath was removed and the reaction mixture stirred at rt for 15 min. Ester **1a**, **1e** or **1i** (1 eq.) was dissolved in pyridine (1 mL) and added *via* micropipette. The mixture was stirred at 50 °C (rt in the synthesis of **4d**), and the reaction was quenched by addition of water after 18–96 h (18 h: **5d**, 20 h: **5a** and **5b**, 72 h: **3a**, **3c**, **3d** and **5c**, 96 h: **4d**). The crude reaction mixture was concentrated at reduced pressure and the product isolated by preparative RP-HPLC.

1,5-Dimethyl-N-(pyridin-3-yl)-1H-pyrazole-3-carboxamide (3a). Compound **1a** (20 mg, 0.119 mmol) yielded **3a** (8.1 mg, 32%, UV purity: 91%) as a colourless solid: Mp 124–127 °C; ¹H NMR (300 MHz, CDCl₃) δ 9.41 (s, 1 H), 9.30 (s, 1 H), 8.91 (d, 1 H), 8.45 (s, 1 H), 7.77 (s, 1 H), 6.66 (s, 1 H), 3.85 (s, 3 H), 2.33 (s, 3 H); ¹³C NMR (75 MHz, CDCl₃) δ 160.9, 143.5, 141.6, 138.6, 136.4, 133.8, 133.3, 126.8, 107.0, 37.0, 11.4; HRMS (M + H)⁺ calcd. for C₁₁H₁₃N₄O⁺ 217.1084, found 217.1082.

1,5-Dimethyl-N-(4H-1,2,4-triazol-3-yl)-1H-pyrazole-3-carboxamide (3c). Compound **1a** (20 mg, 0.119 mmol) yielded **3c** (6.4 mg, 26%, UV purity: 98%) as a colourless solid: Mp >230 °C (decomp.); ¹H NMR (300 MHz, *d*₆-DMSO) δ 10.94 (br s, 1 H), 8.01 (br s, 1 H), 6.68 (s, 1 H), 3.83 (s, 3 H), 2.31 (s, 3 H); ¹³C NMR (75 MHz, *d*₆-DMSO) δ 160.0, 158.4, 157.9, 146.9, 140.8, 106.3, 36.6, 10.7; HRMS (M + H)⁺ calcd. for C₈H₁₁N₆O⁺ 207.0989, found 207.0977.

1,5-Dimethyl-N-((tetrahydrofuran-2-yl)methyl)-1H-pyrazole-3-carboxamide (3d). Compound **1a** (20 mg, 0.119 mmol) yielded **3d** (22.6 mg, 85%, UV purity: 92%) as a light brown oil; ¹H NMR (300 MHz, CDCl₃) δ 7.13 (br s, 1 H), 6.52 (br s, 1 H), 4.08–4.00 (m, 1 H), 3.92–3.85 (m, 1 H), 3.79–3.72 (m, 4 H), 3.70–3.62 (m, 1 H), 3.38–3.30 (m, 1 H), 2.26 (s, 3 H), 2.04–1.81 (m, 3 H), 1.66–1.55 (m, 1 H); ¹³C NMR (75 MHz, CDCl₃) δ 162.6, 145.0, 140.2, 140.2, 106.1, 78.0, 68.3, 42.8, 36.6, 28.8, 26.0, 11.4; HRMS (M + H)⁺ calcd. for C₁₁H₁₈N₃O₂⁺ 224.1394, found 224.1398.

1-Methyl-5-phenyl-N-((tetrahydrofuran-2-yl)methyl)-1H-pyrazole-3-carboxamide (4d). Compound **1e** (20 mg, 0.87 mmol) yielded **4d** (10.2 mg, 41%, UV purity: 80%) as a colourless oil; ¹H NMR (300 MHz, CDCl₃) δ 7.50–7.38 (m, 5 H), 7.22 (br s, 1 H), 6.83 (s, 1 H), 4.12–4.04 (m, 1 H), 3.96–3.91 (m, 1 H), 3.88 (s, 3 H), 3.85–3.68 (m, 2 H), 3.44–3.35 (m, 1 H), 2.08–1.84 (m, 3 H), 1.70–1.59 (m, 1 H); ¹³C NMR (75 MHz, CDCl₃) δ 162.4, 145.5, 145.5, 130.1, 129.0–128.9 (5C) 106.8, 78.1, 68.3, 42.9, 38.1, 28.9, 26.1; HRMS (M + H)⁺ calcd. for C₁₆H₂₀N₃O₂⁺ 286.1550, found 286.1562.

5-Methyl-N-(pyridin-3-yl)-1H-pyrazole-3-carboxamide (5a). Ethyl 3-methyl-1H-pyrazole-5-carboxylate (**1i**) (20 mg, 0.130 mmol) yielded **5a** (24.2 mg, 92%, UV purity: 96%) as a colourless oil; ¹H NMR (300 MHz, *d*₆-DMSO) δ 10.69 (s, 1 H), 9.26 (d, 1 H, *J* 2.4), 8.60 (ddd, 1 H, *J* 1.2, 2.4, 8.4), 8.50 (dd,

1 H, *J* 1.2, 5.1), 7.77 (dd, 1 H, *J* 5.4, 8.7), 6.60 (s, 1 H), 2.33 (s, 3 H); ¹³C NMR (75 MHz, *d*₆-DMSO) δ 161.1, 145.4, 141.0, 139.6, 137.3, 136.6, 131.7, 125.5, 105.0, 10.4; HRMS (M + H)⁺ calcd. for C₁₀H₁₁N₄O⁺ 203.0927, found 203.0924.

5-Methyl-N-(thiazol-2-yl)-1H-pyrazole-3-carboxamide (5b). Ethyl 3-methyl-1H-pyrazole-5-carboxylate (**1i**) (20 mg, 0.130 mmol) yielded **5b** (8.6 mg, 32%, UV purity: 96%) as a colourless solid: Mp >230 °C; ¹H NMR (300 MHz, *d*₆-DMSO) δ 11.85 (br s, 1 H), 7.52 (d, 1 H, *J* 3.6), 7.24 (d, 1 H, *J* 3.6), 6.73 (s, 1 H), 2.29 (s, 3 H); ¹³C NMR (75 MHz, *d*₆-DMSO) δ 159.5, 157.7, 143.2, 141.6, 137.5, 113.6, 105.2, 10.8; HRMS (M + H)⁺ calcd. for C₈H₉N₄O⁺ 209.0492, found 209.0510.

5-Methyl-N-(4H-1,2,4-triazol-3-yl)-1H-pyrazole-3-carboxamide (5c). Ethyl 3-methyl-1H-pyrazole-5-carboxylate (**1i**) (20 mg, 0.130 mmol) yielded **5c** (5.8 mg, 23%, UV purity: 87%) as a colourless solid: Mp >230 °C; ¹H NMR (300 MHz, *d*₆-DMSO) δ 11.04 (br s, 1 H), 8.05 (br s, 1 H), 6.67 (s, 1 H), 2.28 (s, 3 H); HRMS (M + H)⁺ calcd. for C₇H₉N₆O⁺ 193.0832, found 193.0846.

5-Methyl-N-((tetrahydrofuran-2-yl)methyl)-1H-pyrazole-3-carboxamide (5d). Ethyl 3-methyl-1H-pyrazole-5-carboxylate (**1i**) (20 mg, 0.130 mmol) yielded **5d** (20.6 mg, 80%, UV purity: 93%) as a colourless solid: Mp 161–162 °C; ¹H NMR (300 MHz, CDCl₃) δ 9.03 (br s, 1 H), 8.44 (br s, 1 H), 4.21–4.13 (m, 1 H), 3.98–3.91 (m, 1 H), 3.86–3.70 (m, 2 H), 3.45–3.36 (m, 1 H), 2.32 (s, 3 H), 2.11–1.89 (m, 3 H), 1.71–1.59 (m, 1 H); ¹³C NMR (75 MHz, CDCl₃) δ 163.2, 147.0, 140.7, 105.4, 79.3, 68.1, 43.0, 28.8, 25.9, 11.1; HRMS (M + H)⁺ calcd. for C₁₀H₁₆N₃O₂⁺ 210.1237, found 210.1226.

Acknowledgements

This work was supported by the Danish Cancer Society (Grant No. 002521109210), the Danish Research Council (Grant No. 21-01-0511), Aase og Ejnar Danielsens Fond, the Lundbeck Foundation (Grant No. 119/14) and by the Villum Kann Rasmussen Foundation (Grant 1002-12).

References

- 1 G. Manning, D. B. Whyte, R. Martinez, T. Hunter and S. Sudarsanam, *Science*, 2002, **298**, 1912–1934.
- 2 M. E. M. Noble, J. A. Endicott and L. N. Johnson, *Science*, 2004, **303**, 1800–1805.
- 3 G. Kéri, L. Örfi, D. Erös, B. Hegymegi-Barakonyi, C. Szántai-Kis, Z. Horváth, F. Wáczek, J. Marosfalvi, I. Szabadkai, J. Pató, Z. Greff, D. Hafenbradl, H. Daub, G. Müller, B. Klebl and A. Ullrich, *Curr. Signal Transduct. Ther.*, 2006, **1**, 67–95.
- 4 B. Li, Y. Liu, T. Uno and N. Gray, *Comb. Chem. High Throughput Screening*, 2004, **7**, 453–472.
- 5 M. Cherry and D. H. Williams, *Curr. Med. Chem.*, 2004, **11**, 663–673.
- 6 P. Furet, T. Meyer, A. Strauss, S. Raccuglia and J.-M. Rondeau, *Bioorg. Med. Chem. Lett.*, 2002, **12**, 221–224.
- 7 M. Ikuta, K. Kamata, K. Fukasawa, T. Honma, T. Machida, H. Hirai, I. Suzuki-Takahashi, T. Hayama and S. Nishimura, *J. Biol. Chem.*, 2001, **276**, 27548–27554.
- 8 M. Ohori, T. Kinoshita, M. Okubo, K. Sato, A. Yamazaki, H. Arakawa, S. Nishimura, N. Inamura, H. Nakajima and M. Neya, *Biochem. Biophys. Res. Commun.*, 2005, **336**, 357–363.
- 9 J. S. Sawyer, D. W. Beight, K. S. Britt, B. D. Anderson, R. M. Campbell, T. Goodson, D. K. Herron, H. Y. Li, W. T. McMillen, N. Mort, S. Parsons, E. C. R. Smith, J. R. Wagner, L. Yan, F. M. Zhang and J. M. Yingling, *Bioorg. Med. Chem. Lett.*, 2004, **14**, 3581–3584.
- 10 J. S. Sawyer, B. D. Anderson, D. W. Beight, R. M. Campbell, M. L. Jones, D. K. Herron, J. W. Lampe, J. R. McCowan, W. T. McMillen,

- N. Mort, S. Parsons, E. C. R. Smith, M. Vieth, L. C. Wier, L. Yan, F. M. Zhang and J. M. Yingling, *J. Med. Chem.*, 2003, **46**, 3953–3956.
- 11 D. Fancelli, D. Berta, S. Bindi, A. Cameron, P. Cappella, P. Carpinelli, C. Catana, B. Forte, P. Giordano, M. L. Giorgini, S. Mantegani, A. Marsiglio, M. Meroni, J. Moll, V. Pittala, F. Roletto, D. Severino, C. Soncini, P. Storici, R. Tonani, M. Varasi, A. Vulpetti and P. Vianello, *J. Med. Chem.*, 2005, **48**, 3080–3084.
- 12 B. Guerra and O.-G. Issinger, *Electrophoresis*, 1999, **20**, 391–408.
- 13 D. W. Parsons, T.-L. Wang, Y. Samuels, A. Bardelli, J. M. Cummins, L. DeLong, N. Silliman, J. Ptak, S. Szabo, J. K. V. Willson, S. Markowitz, K. W. Kinzler, B. Vogelstein, C. Lengauer and V. E. Velculescu, *Nature*, 2005, **436**, 792.
- 14 B. S. Skålhegg and K. Tasken, *Front. Biosci.*, 2000, **5**, D678–D693.
- 15 A. Basu, *Pharmacol. Ther.*, 1993, **59**, 257–280.
- 16 P. P. Roux and J. Blenis, *Microbiol. Mol. Biol. Rev.*, 2004, **68**, 320–344.
- 17 J. Regan, A. Capolino, P. F. Cirillo, T. Gilmore, A. G. Graham, E. Hickey, R. R. Kroe, J. R. Madwed, M. Moriak, R. Nelson, C. A. Pargellis, A. Swinamer, C. Torcellini, M. Tsang and N. Moss, *J. Med. Chem.*, 2003, **46**, 4676–4686.
- 18 J. Regan, S. Breitfelder, P. Cirillo, T. Gilmore, A. G. Graham, E. Hickey, B. Klaus, J. Madwed, M. Moriak, N. Moss, C. Pargellis, S. Pav, A. Proto, A. Swinamer, L. Tong and C. Torcellini, *J. Med. Chem.*, 2002, **45**, 2994–3008.
- 19 M. Rinaldi-Carmona, F. Barth, J. Millan, J.-M. Derocq, P. Casellas, C. Congy, D. Oustric, M. Sarran, M. Bouaboula, B. Calandra, M. Portier, D. Shire, J.-C. Breliere and G. L. Fur, *J. Pharmacol. Exp. Ther.*, 1998, **284**, 644–650.
- 20 T. Persson and J. Nielsen, *Org. Lett.*, 2006, **8**, 3219–3222.
- 21 A. Basha, M. Lipton and S. M. Weinreb, *Tetrahedron Lett.*, 1977, **18**, 4171–4174.
- 22 J. I. Levin, E. Turos and S. M. Weinreb, *Synth. Commun.*, 1982, **12**, 989–993.
- 23 M. F. Lipton, A. Basha and S. M. Weinreb, *Org. Synth.*, 1988, **59**, 492–495.
- 24 C. Pargellis, L. Tong, L. Churchill, P. F. Cirillo, T. Gilmore, A. G. Graham, P. M. Grob, E. R. Hickey, N. Moss, S. Pav and J. Regan, *Nat. Struct. Biol.*, 2002, **9**, 268–272.
- 25 D. P. Brazil, Z.-Z. Yang and B. A. Hemmings, *Trends Biochem. Sci.*, 2004, **29**, 233–242.
- 26 M. Gómez-Guillén, *Carbohydr. Res.*, 1989, **180**, 1–17.
- 27 C. Kashima, S. Shibata, H. Yokoyama and T. Nishio, *J. Heterocycl. Chem.*, 2003, **40**, 773–782.
- 28 M. Gómez-Guillén, F. Hans-Hans, J. M. L. Simon and M. E. Martín-Zamora, *Carbohydr. Res.*, 1989, **189**, 349–358.
- 29 G. V. Boyd and K. Heatheri, *J. Chem. Soc., Perkin Trans. 1*, 1973, 2532–2535.